PPARγ1 attenuates cytosol to membrane translocation of PKCα to desensitize monocytes/macrophages

Andreas von Knethen, Mathias Soller, Nico Tzieply, Andreas Weigert, Axel M. Johann, Carla Jennewein, Roman Köhl, and Bernhard Brüne

Institute of Biochemistry I, Faculty of Medicine, Johann Wolfgang Goethe University, 60590 Frankfurt, Theodor-Stern-Kai 7, Germany

Recently, we provided evidence that PKCα depletion in monocytes/macrophages contributes to cellular desensitization during sepsis. We demonstrate that peroxisome proliferator–activated receptor γ (PPARγ) agonists dose dependently block PKCα depletion in response to the diacylglycerol homologue PMA in RAW 264.7 and human monocyte–derived macrophages. In these cells, we observed PPARγ-dependent inhibition of nuclear factor-κB (NF-κB) activation and TNF-α expression in response to PMA. Elucidating the underlying mechanism, we found PPARγ1 expression not only in the nucleus but also in the cytoplasm. Activation of PPARγ1 wild type, but not an agonist-binding mutant of PPARγ1, attenuated PMA-mediated PKCα cytosol to membrane translocation. Coimmunoprecipitation assays pointed to a protein–protein interaction of PKCα and PPARγ1, which was further substantiated using a mammalian two-hybrid system. Applying PPARγ1 mutation and deletion constructs, we identified the hinge helix 1 domain of PPARγ1 that is responsible for PKCα binding. Therefore, we conclude that PPARγ1-dependent inhibition of PKCα translocation implies a new model of macrophage desensitization.

Introduction

Monocyte/macrophage desensitization is characteristic for late-phase immune responses (Liew et al., 2005). Confined proinflammatory cytokine expression and mediator synthesis is important to avoid pathological settings, such as sepsis or atherosclerosis (Hotchkiss and Karl, 2003; Hansson, 2005). Down-regulating proinflammatory cytokine expression (TNF-α, interleukin [IL]-1β, and IFNγ) or proinflammatory mediator release (nitric oxide and reactive oxygen species [ROS]) concomitantly switches the proinflammatory phenotype toward an antiinflammatory one. The latter is characterized by the synthesis of antiinflammatory cytokines, such as TGF-β or IL-10, and is often accompanied by cellular desensitization upon secondary proinflammatory stimulation (Docke et al., 1997; Kalechman et al., 2002). Therefore, the identification of molecular mechanisms contributing to cellular desensitization attracted growing interest (Docke et al., 1997; von Knethen and Brune, 2002).

One factor attenuating proinflammatory gene expression is peroxisome proliferator–activated receptor (PPARγ). PPARγ is a nuclear hormone receptor that, upon agonist binding, transactivates gene expression as a heterodimer bound to retinoic acid receptor-α (Abdelrahman et al., 2005). Its role in blocking proinflammatory gene expression comprises several options, mainly antagonizing signaling cascades. Specifically, PPARγ negatively regulates transcription factors by scavenging transcriptional coactivators, such as the cAMP-response element–binding protein or the steroid receptor coactivator-1 (Yang et al., 2000). However, a direct association with the transcription factors NF-κB, NF of activated T cells, signal transducer, and activator of transcription or NF-E2–related factor 2 (Ikeda et al., 2000; Wang et al., 2001, 2004; Chung et al., 2003) blocks their recruitment to responsive elements in promoter structures of target genes. Recently, it has been shown that PPARγ is targeted to nuclear receptor corepressor–histone deacetylase-3 complexes in response to ligand-dependent SUMOylation (Pascual et al., 2005), protecting these complexes from proteosomal degradation. Normally, histone deacetylase-3 removes a corepressor complex, provoking expression of proinflammatory genes. Additionally, PPARγ represses activation of a mitogen-activated protein kinase, which keeps downstream transcription factors

Correspondence to Andreas von Knethen: v_knethen@zbc.kgu.de

Abbreviations used in this paper: 15d-PGJ$_2$, 15-deoxy-$\Delta^{12,14}$-prostaglandin J$_2$; AF, activating function; CHX, cycloheximide; DAG, diacylglycerol; DBD, DNA-binding domain; DGKα, DAG kinase α; EMSA, electrophoretic mobility shift assay; HEK, human embryonic kidney; IL, interleukin; LBD, ligand-binding domain; MCS, multicloning site; NF-κB, nuclear factor-κB; PPARγ, peroxisome proliferator–activated receptor γ; ROS, reactive oxygen species.

The Journal of Cell Biology, Vol. 176, No. 5, February 26, 2007 681–694
http://www.jcb.org/cgi/doi/10.1083/jcb.200605038

unphosphorylated and, consequently, inactive (Desreumaux et al., 2001). Moreover, PPARγ influences the cell cycle by up-regulating p21 expression, which is an established cell cycle inhibitor (Han et al., 2004), or down-regulating phosphatase PPA2, which is known to adjust E2F/DP DNA-binding activity, which is necessary for the G_1 to S-phase transition (Altiok et al., 1997). In response to proinflammatory stimulation, PPARγ-dependent gene transcription also contributes to cellular desensitization. PPARγ agonists inhibit diacylglycerol (DAG)–PKC signaling by inducing DAG kinase-α (DGKα) expression (Verrier et al., 2004). This enzyme lowers the amount of DAG, which is an established PKC activator. Normally, DAG is released from membrane lipids and activates classical PKCs (Liu and Heckman, 1998). Based on gene induction of DGKα as the underlying mechanism, this type of desensitization demands at least 6–15 h. Thus, it appears that PPARγ transrepresses proinflammatory gene expression, often in a DNA-unbound state, by provoking direct protein–protein interactions.

We provide evidence for a new PPARγ-dependent mechanism in blocking PKCα signaling. Depletion of PKCα is attenuated by PPARγ1 activation in RAW 264.7 cells or human primary monocyte–derived macrophages. Cytosolic localization of PPARγ1 interferes with PKCα cytosol to membrane translocation, which is a prerequisite for its activation-dependent depletion. Translocation is restored in cells transfected with a dominant-negative PPARγ1 mutant. Coimmunoprecipitation studies and a mammalian two-hybrid system revealed a direct PPARγ1–PKCα interaction as the underlying mechanism. PPARγ1 deletion constructs support the idea that ligand-dependent PPARγ activation is necessary for PKCα binding, which is mediated by the helix 1 of the PPARγ1 hinge domain. Our data suggest a new mechanism for how activation of PPARγ1 blocks PKCα translocation, thereby achieving cellular desensitization.

Results

PPARγ agonists inhibit PKCα depletion

Recent data demonstrate that monocyte/macrophage desensitization in response to phagocytosis of apoptotic cells is achieved by attenuating PKCα signaling, which blocks NADPH oxidase–dependent formation of ROS (Johann et al., 2006). Therefore, we were interested in identifying molecular mechanisms interfering with PKCα depletion. A potential candidate known to affect the pro- versus antiinflammatory phenotype in monocytes/macrophages is PPARγ. Because controversial data exist concerning its expression in monocytic and macrophage cell lines, as well as in primary human monocytes and macrophages, we performed a first set of experiments determining PPARγ expression in the monocytic cell lines and primary cells under investigation. As shown in Fig. 1 A, PPARγ is constitutively expressed in murine RAW 264.7 macrophages. In contrast, in THP-1 cells, PPARγ is only fractionally expressed, but differentiation toward macrophages with 100 nM PMA for 24 h provoked up-regulation of PPARγ (Fig. 1 A, lane 2 vs. 3). A similar expression pattern is observed in primary monocytes and macrophages, respectively. PPARγ is only marginally expressed in

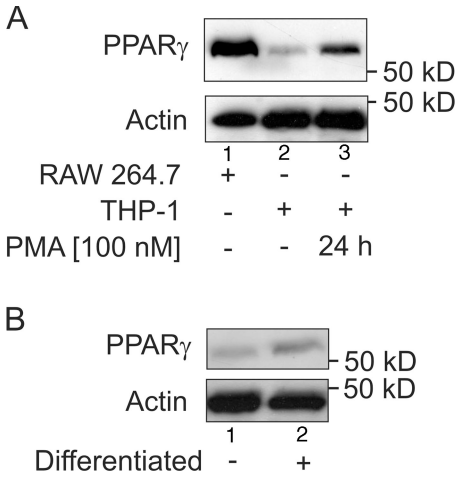

Figure 1. **PPARγ expression in monocytes/macrophages.** (A) PPARγ expression was determined in lysates of RAW 264.7 macrophages and in control versus differentiated THP-1 cells. For differentiation, cells were treated for 24 h with 100 nM PMA. Western blot was performed as described in Materials and methods. (B) PPARγ expression was analyzed by Western analysis in primary human monocytes and macrophages, differentiated for 7 d with medium containing serum of AB-positive donors. Experiments were performed at least three times, and representative data are shown.

monocytes, but induced upon differentiation toward macrophages (Fig. 1 B). To identify the expressed PPARγ isoform 1 or 2, we performed a Western blot using human PPARγ1-transfected human embryonic kidney (HEK) cells as a positive control. Taking into consideration that murine and human PPARγ1 are identical in size (475 aa), we conclude that PPARγ1 is expressed in RAW 264.7 macrophages, differentiated THP-1 cells, and primary macrophages (unpublished data). Based on these results, we choose RAW 264.7 cells, differentiated human THP-1 cells, and primary monocyte–derived macrophages as experimental cell models.

To analyze the role of PPARγ in macrophages in affecting PKCα activation, we pretreated RAW 264.7 macrophages for 1 h with the PPARγ agonists ciglitazone and rosiglitazone, followed by the addition of 100 nM PMA, which is a DAG homologue and established activator of PKCα. As expected, PKCα depletion was observed in control cells in response to 100 nM PMA (Fig. 2 A, lane 2). Depletion of PKCα was attenuated in cells prestimulated with a PPARγ agonist, such as ciglitazone (Fig. 2 A, lanes 3 and 4) or rosiglitazone (Fig. 2 A, lanes 5 and 6), in a concentration-dependent manner. However, 1 μM PMA-mediated PKCα depletion was not blocked (unpublished data). From these data, we conclude that PPARγ agonists attenuate activation-dependent PKCα depletion, in part controlled by the magnitude of the PKCα–activating stimulus. In PPARγ1 activating function (AF) 2 mutant overexpressing RAW 264.7 macrophages (Johann et al., 2006), pretreatment with 10 μM rosiglitazone or 10 μM ciglitazone did not inhibit PKCα depletion in response to PMA (Fig. 2 B).

Because a 1-h prestimulation period is short for gene expression and protein synthesis, we hypothesized that preserved PKCα expression did not require protein synthesis. To prove this assumption, we added the established translation inhibitor cyclohexamide (CHX) 1 h before PPARγ agonist stimulation

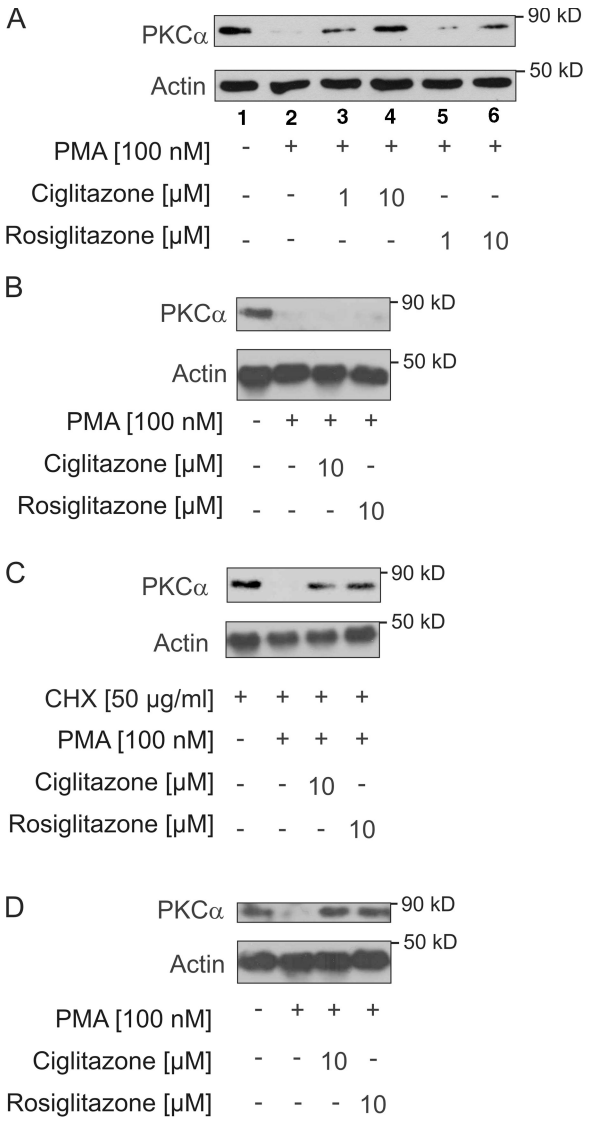

Figure 2. **PPARγ agonist prestimulation inhibits PKCα depletion.** RAW 264.7 macrophages (A) and PPARγ1 AF2–overexpressing RAW 264.7 cells (B) were prestimulated for 1 h with ciglitazone (1 or 10 μM), rosiglitazone (1 or 10 μM), or remained as controls, followed by the addition of 100 nM PMA for 1 h. (C) RAW 264.7 macrophages were stimulated for 1 h with 50 μg/ml CHX. Thereafter, 10 μM of rosiglitazone or ciglitazone were added for 1 h, followed by 100 nM PMA stimulation for 1 h. (D) Primary monocyte–derived macrophages were prestimulated for 1 h with 10 μM ciglitazone, 10 μM rosiglitazone, or remained as controls. Afterward, 100 nM PMA was added for 1 h. For all experiments, cells were harvested and lysed, and Western blot was performed as described in the Materials and methods. Experiments were performed at least three times, and representative data are shown.

(Fig. 2 C). As expected, blocking translation with CHX did not interfere with the ability of PPARγ agonists to block PKCα depletion, suggesting a translation-independent mode of action.

The physiological significance of these results obtained in murine RAW 264.7 macrophages was verified in primary human monocyte–derived macrophages isolated from peripheral blood. Similar to RAW 264.7 cells, in primary macrophages, pretreatment with ciglitazone and rosiglitazone preserved PKCα expression upon PMA addition (Fig. 2 D).

Antiinflammatory consequences of PPARγ1–PKCα interaction

To elucidate whether the PPARγ1–PKCα interaction shows an impact on PKCα signaling in inflammatory gene expression in macrophages, we analyzed two proinflammatory markers of macrophage activation, i.e., NF-κB DNA binding and TNF-α expression in response to PMA in RAW 264.7 macrophages. To determine activation of the proinflammatory transcription factor NF-κB, we performed a set of electrophoretic mobility shift assays (EMSAs), demonstrating the DNA-binding capability of the transcription factor. As shown in Fig. 3 A, 100 nM PMA supplied for 3 h significantly induced NF-κB activation (Fig. 3 A, second lane) compared with the untreated control (Fig. 3 A, first lane). To elucidate the composition of the transcription factor complex, we used antibodies against the p50 (Fig. 3 B, left) and p65 subunits (Fig. 3 B, right) of NF-κB. As shown in Fig. 3 B (left), the lower and the upper NF-κB shifts contained the p50 subunit. Therefore, the two bands were significantly reduced when an α-p50 antibody was included in the binding reaction and a new band, the p50 supershift, occurred. Only the upper NF-κB shift included the p65-subunit, as indicated by the addition of the α-p65 antibody, which provoked the reduction of the upper NF-κB shift, but did not alter the lower NF-κB shift (Fig. 3 B, right). As expected, a new band was detectable (the p65 supershift). Thus, we conclude that the lower NF-κB shift is formed by a p50 homodimer, whereas the upper NF-κB shift consists of a p50/p65 heterodimer.

To identify whether activation of NF-κB complexes is influenced by PPARγ activation, we treated RAW 264.7 cells with the natural PPARγ agonist 15-deoxy-$\Delta^{12,14}$-prostaglandin J_2 (15d-PGJ_2; Kobayashi et al., 2005; Rogler, 2006). Taking into consideration that 15d-PGJ_2 may also act PPARγ independently on NF-κB activation (Straus et al., 2000), we included the PPARγ antagonist GW9662 in this experiment (Leesnitzer et al., 2002). This allowed us to discover to what extent 15d-PGJ_2 affected PMA-mediated NF-κB activation PPARγ dependently. As depicted in Fig. 3 C, pretreatment of RAW 264.7 cells with 10 μM 15d-PGJ_2 for 1 h reduced the p50/p65 heterodimer formation in response to PMA (Fig. 3 C, second lane) compared with PMA-treated controls (Fig. 3 C, first lane). Preincubation of the cells for 1 h with 10 μM GW9662 completely eliminated the influence of 15d-PGJ_2 on NF-κB activation (Fig. 3 C, right lane). To show that these results are not restricted to our cell line model, we performed a similar EMSA using nuclear extracts isolated from primary human macrophages. In primary cells, 10 μM of the natural PPARγ agonist 15d-PGJ_2 inhibits 100 nM PMA-mediated NF-κB activation (Fig. 3 D, middle lane), which is restored after 10 μM GW9662 pretreatment for 1 h (Fig. 3 D, right lane). However, in human macrophages, only one NF-κB shift in response to PMA, which is formed by a p50/p65 heterodimer (unpublished data), is observed. From these results, we reasoned that PPARγ activation reduced the NF-κB DNA-binding ability in response to PMA by ∼50% compared with PMA-treated controls. To determine whether reduced NF-κB activation modulates expression of proinflammatory cytokines, we finally examined TNF-α expression of RAW 264.7 macrophages in response to PMA. TNF-α expression was determined

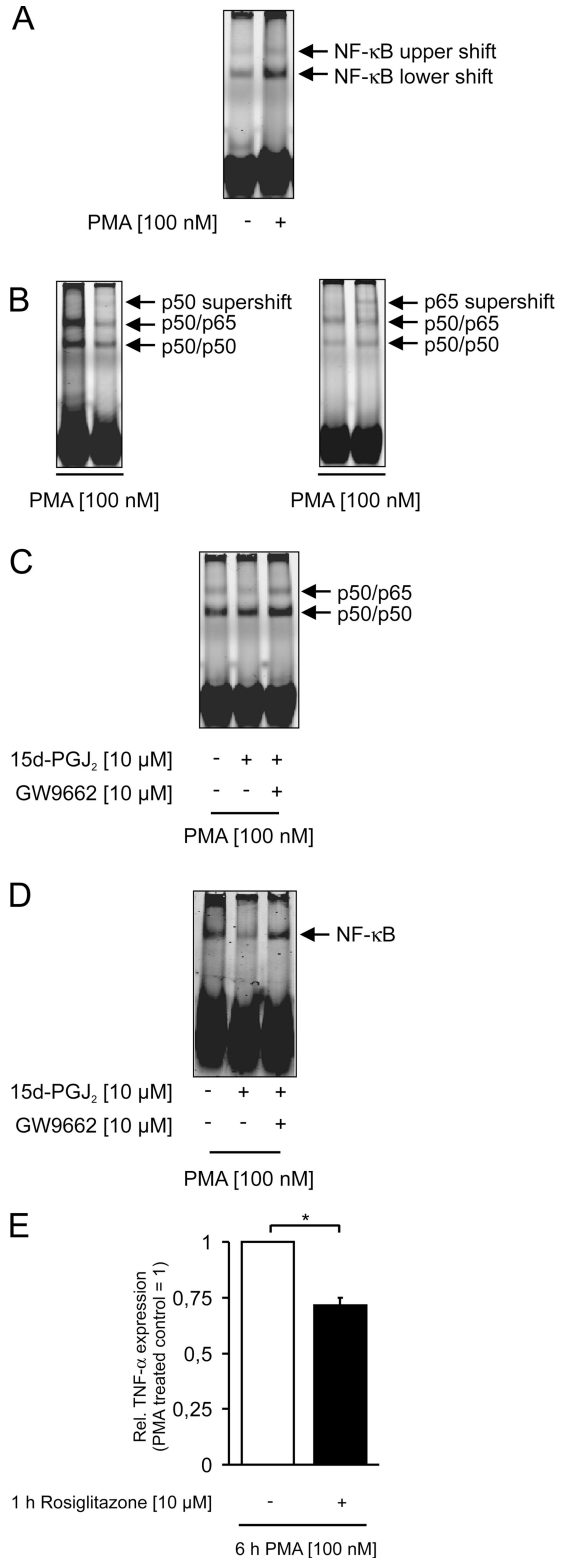

Figure 3. **PPARγ1-dependent attenuation of PKCα translocation provokes a reduction of the proinflammatory response in macrophages.** (A) Activation of NF-κB in RAW 264.7 macrophages in response to PMA. RAW 264.7 macrophages were stimulated for 3 h with 100 nM PMA or left untreated as control. Afterward, cells were harvested, nuclear extracts were isolated, and NF-κB EMSA was performed as described in the Materials and methods. (B) Supershift analysis of the active NF-κB complex was described in the Materials and methods. Macrophages were stimulated with 100 nM PMA for 3 h. For supershift analysis, a p50 antibody (left, second lane) or a p65 antibody (right, second lane) was included. NF-κB activation without antibody addition (left and right, first lane) is shown. (C) 15d-PGJ_2 inhibited PMA-mediated NF-κB activation. RAW 264.7 cells were pretreated with 10 μM of the endogenous PPARγ ligand 15-dPGJ_2 for 1 h, followed by the addition of 100 nM PMA for 3 h (middle lane). To ensure a PPARγ-dependent effect, one sample was prestimulated before 15d-PGJ_2 addition with 10 μM of the PPARγ antagonist GW9662 for 1 h (right lane). One sample remained PMA treated only as a control (left lane). Cells were harvested, nuclear protein extracts were isolated, and NF-κB EMSA was performed as described in Materials and methods. (D) PMA-mediated NF-κB activation is inhibited in human primary macrophages in response to 15d-PGJ_2. Primary monocyte–derived macrophages were treated as described in C. Cells were harvested and processed, and NF-κB EMSA was performed as described in Materials and methods. (E) Inhibition of PMA-mediated PKCα activation by PPARγ reduced proinflammatory TNF-α expression. RAW 264.7 cells were treated for 1 h with 10 μM rosiglitazone or remained as controls. Afterward, cells were incubated with 100 nM PMA for 6 h, and TNF-α expression in the cell supernatant was analyzed using the CBA system. All experiments were performed at least three times. Data are the means ± the SD of the individual experiments (*, $P < 0.05$) or representative of three similar experiments.

by the cytometric bead array using a FACSCanto flowcytometer. As shown in Fig. 3 E, pretreatment of RAW 264.7 macrophages for 1 h with 10 μM rosiglitazone before addition of 100 nM PMA for 6 h reduced PMA-mediated TNF-α expression to ∼70%. These results suggest that activated PPARγ1 inhibits PKCα-dependent signaling in macrophages, thereby provoking, at least in part, an attenuated proinflammatory gene expression profile in association with cellular desensitization.

PPARγ1-dependent inhibition of PKCα translocation

Considering that activation of PKCα, followed by its translocation to the cell membrane, is a prerequisite for its depletion, we were interested to determine whether PPARγ blocks PKCα translocation. To follow PPARγ and PKCα distribution in RAW 264.7 cells, we stained for PPARγ and PKCα in paraformaldehyde-fixed cells (Fig. 4). As shown in Fig. 4 A (third panel), PPARγ localizes in the cytosol and the nucleus in untreated cells, whereas PKCα is localized in the cytosol (Fig. 4 A, second panel). The nucleus is counterstained, using DAPI (Fig. 4 A, first panel), and an overlay is provided in Fig. 4 A (fourth panel). To prove specificity of the secondary antibodies used, which were labeled with either Alexa Fluor 488 or 546, we used these antibodies alone without a first antibody. In both cases, no signal is observed (unpublished data). Activation of the cells with 100 nM PMA for 50 min provokes PKCα translocation (Fig. 4 B, second panel), whereas localization of PPARγ is not altered (Fig. 4 B, third panel). Pretreatment of RAW 264.7 macrophages with 10 μM of the synthetic PPARγ agonist rosiglitazone for 1 h prevents PKCα translocation in response to 100 nM PMA stimulation for 50 min (Fig. 4 C, second panel). Localization of PPARγ remains unaltered (Fig. 4 C, third panel). To prove a PPARγ-dependent effect, we used the PPARγ-specific antagonist GW9662. Preincubation of the cells for 1 h with 10 μM GW9662, followed by rosiglitazone treatment (1 h, 10 μM), restores PKCα translocation after 100 nM PMA addition for 50 min (Fig. 4 D, second panel). PPARγ localization was not affected (Fig. 4 D, third panel). From these data, we conclude that activated cytosolic PPARγ in RAW 264.7 macrophages inhibits

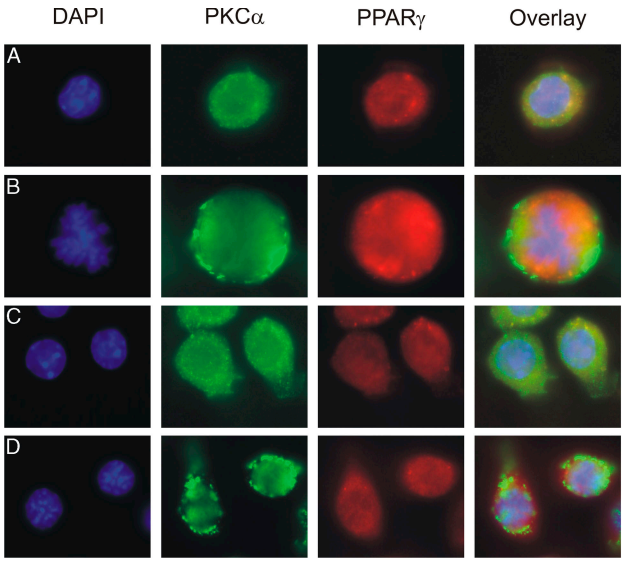

Figure 4. **PKCα and PPARγ localization in RAW 264.7 macrophages.** To follow PKCα and PPARγ localization in RAW 264.7 macrophages, cells were seeded on slides and treated (B) for 50 min with 100 nM PMA, (C) preincubated with 10 μM rosiglitazone for 1 h followed by 100 nM PMA addition for 50 min, or (D) pretreated with 10 μM GW9662 before cells were stimulated as described in C. Afterward, cells were fixed and stained for PKCα and PPARγ as described in the Materials and methods. Cell nuclei were counterstained with DAPI. DAPI staining is shown in the first panel, PKCα staining in the second, PPARγ staining in the third, and an overlay to estimate cytosolic and nuclear region is provided in the fourth panel. All experiments were performed three times, and representative data are shown.

PKCα translocation in response to 100 nM PMA. Based on the aforementioned Western blot results, RAW 264.7 cells express isoform 1, which is partially located in the cytosol.

To verify the impact of PPARγ1 activation on PKCα translocation, we used HEK293 cells. Cells were transiently transfected with a PPARγ1 wild-type–encoding vector, tagged with DsRed-monomer or a DsRed-monomer–tagged PPARγ1 AF2 mutant–encoding vector in combination with a PKCα-EGFP–encoding vector. The PPARγ1 AF2 mutant contains two amino acid exchanges (L468A/E471A), thus preventing ligand binding and concomitant PPARγ1 activation (Gurnell et al., 2000). To follow PKCα translocation, 100 nM PMA was added to rosiglitazone-pretreated and control cells. Changes in PKCα localization were documented 1 h after rosiglitazone stimulation and 50 min after 100 nM PMA addition. PMA provokes PKCα-EGFP translocation to the cell membrane in DsRed-tagged PPARγ1 wild type, as well as DsRed-tagged PPARγ AF2 mutant–expressing cells, as expected (Fig. 5 A, second row, second panel vs. fourth row, second panel). Localization of PPARγ does not change (Fig. 5 A, first row, third panel vs. second row, third panel; and third row, third panel vs. fourth row, third panel). In cells transfected with the DsRed-tagged PPARγ1 wild-type construct, rosiglitazone pretreatment inhibited PKCα-EGFP translocation to the cell membrane in response to PMA (Fig. 5 B, second row, second panel), whereas in cells transfected with the DsRed-tagged PPARγ AF2 mutant, rosiglitazone preincubation does not prevent PKCα-EGFP translocation (Fig. 5 B, fourth row, second panel). However, PPARγ localization remains unaltered in all analyzed samples (Fig. 5, A and B, first through fourth row, third panel). As shown in Fig. 5 C, preincubation of the cells with the PPARγ antagonist GW9662 (10 μM) for 1 h, completely abolished the PPARγ-dependent inhibition of PKCα translocation in response to PMA (bottom row, second panel). Inline pretreatment of the cells with the PPARα agonist WY14643 (10 μM) for 1 h did not inhibit PMA-mediated PKCα translocation (Fig. 5 D, bottom row, second panel), which further approved a PPARγ-dependent effect. In corroboration with Fig. 5 (A and B), PPARγ localization was unaffected in response to GW9662 or WY14643 and PMA treatment (Fig. 5, C and D, first and second row, third panel).

Based on these findings, we went on to analyze whether PPARγ1 inhibits PKCα translocation by a direct protein–protein interaction.

PPARγ1 directly binds to PKCα

To elucidate whether PPARγ1 inhibits PKCα translocation by a direct PPARγ1–PKCα interaction, we performed a set of coimmunoprecipitation experiments. Immunoprecipitation of PKCα from lysates of differentiated THP-1 cells, which had been stimulated for 1 h with rosiglitazone or left untreated, was conducted. As shown in Fig. 6 A, immunoprecipitation of PKCα resulted in coimmunoprecipitation of PPARγ1 in THP-1 cells that had been challenged with a PPARγ agonist (Fig. 6 A, lane 2). In the flowthrough, PPARγ1 was only detected when agonist stimulation was omitted (Fig. 6 A, lane 1). After PPARγ1 activation, PPARγ1 was almost completely retarded in the immunoprecipitation column.

To verify a PPARγ1-dependent mechanism, we transfected COS-7 cells with PPARγ1 wild-type or AF2-encoding plasmids and a PKCα-EGFP expression plasmid. Immunoprecipitation was performed using μMacs anti-GFP beads. In cells transfected with the PPARγ1 AF2 mutant, little if any PPARγ1 coimmunoprecipitated with PKCα-EGFP in response to 10 μM rosiglitazone (Fig. 6 B, lane 4). In cells transfected with the PPARγ1 wild-type plasmid, rosiglitazone treatment allowed to coimmunoprecipitate PPARγ1 with PKCα-EGFP (Fig. 6 B, lane 2), pointing to the importance of agonist activation to promote PKCα binding.

To provide further evidence for a direct PPARγ1–PKCα interaction, we used the mammalian two-hybrid system. In COS-7 cells transiently transfected by electroporation with a combination of pCMV-AD-PPARγ1, pCMV-BD-PKCα, and the Gal4 reporter vector pFR-luc, addition of rosiglitazone or ciglitazone provoked induction of luciferase expression as determined by a luciferase assay. As shown in Fig. 7, addition of both PPARγ agonists induce luciferase expression roughly threefold compared with untreated controls. A PPARγ-dependent effect was verified because addition of the PPARα agonist

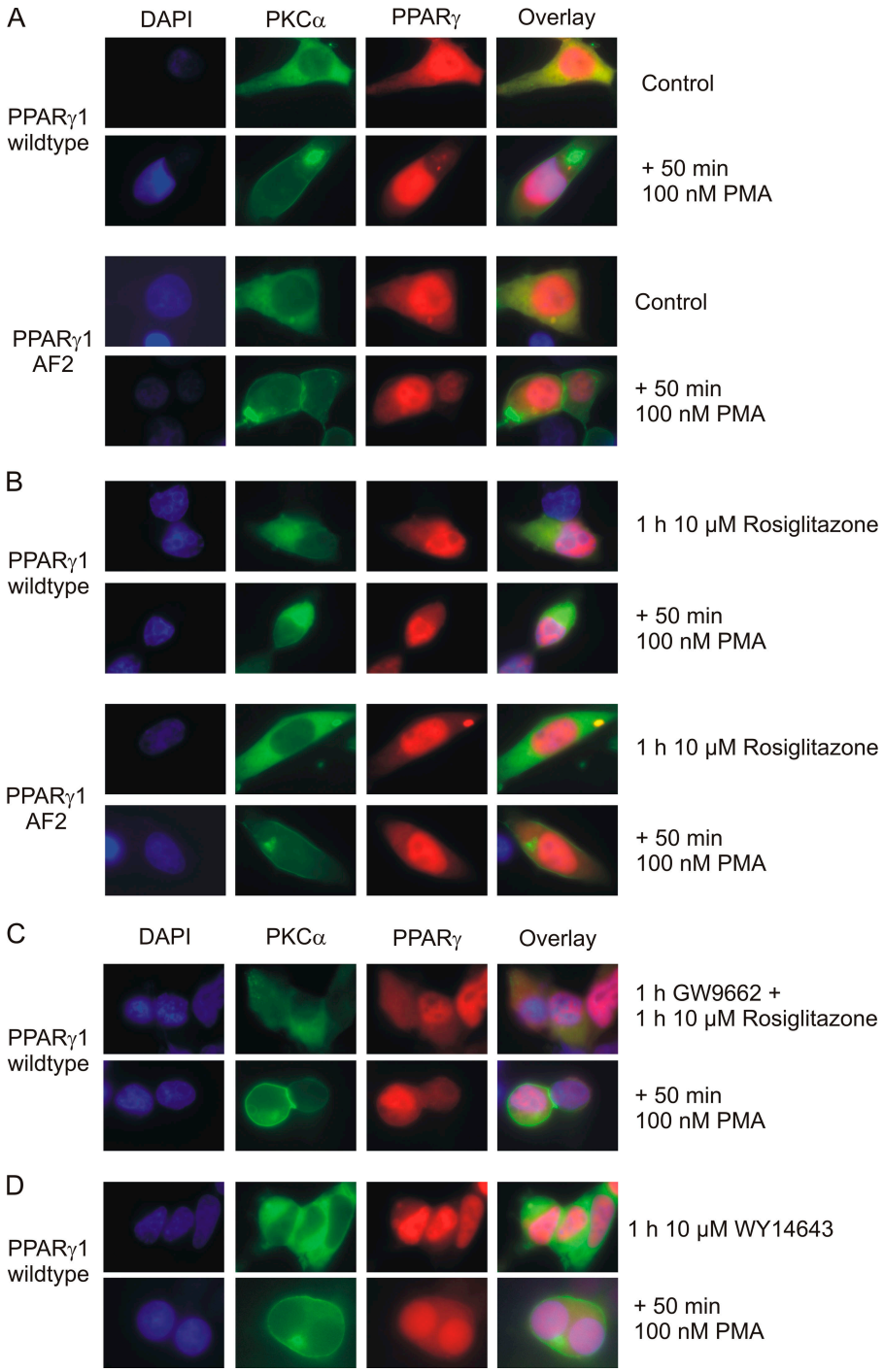

Figure 5. **PPARγ1 inhibits PKCα translocation.** HEK293 cells were cotransfected with DsRed-PPARγ1 wild type/PKCα-EGFP (A and B [top two rows] and C and D) or DsRed-PPARγ1 AF2/PKCα-EGFP (A and B, bottom two rows). To follow PKCα-EGFP translocation, 100 nM PMA was added to control cells (A, second and fourth row) or cells pretreated for 1 h with 10 μM rosiglitazone (B, second and fourth row). To verify the role of PPARγ on PKCα-EGFP translocation in DsRed-PPARγ1 wild type/PKCα-EGFP, cotransfected HEK293 cells were treated for 1 h with 10 μM of the PPARγ antagonist GW9662 before stimulation for 1 h with 10 μM rosiglitazone (C, top row) followed by 50 min of 100 nM PMA addition (C, bottom row) or preincubated for 1 h with 10 μM of the PPARα agonist WY14643 (D, top row) before activation with 100 nM PMA for 50 min (D, bottom row). Cell nuclei were counterstained with DAPI. DAPI staining is shown in the first panel, PKCα-EGFP in the second, DsRed-PPARγ in the third, and an overlay to estimate cytosolic and nuclear region is provided in the fourth panel. All experiments were performed three times, and representative data are shown.

WY14643 left basal luciferase activity unaltered. With this two-hybrid model, direct binding of target (PPARγ1) to bait protein (PKCα) is required to induce luciferase expression. Therefore, our data suggest that PPARγ1 directly binds PKCα upon agonist activation. This interaction inhibits PKCα translocation to the cell membrane, and thus, PKCα activation.

Identification of PPARγ1 domains involved in PKCα binding

To identify PPARγ1 domains that promote binding to PKCα, we first generated a set of point mutations, each substituting one aa in helix 4 of the ligand-binding domain (LBD), taking into consideration that this region is important in binding transcriptional coactivators (Nolte et al., 1998; Westin et al., 1998), and therefore might be responsible for binding to PKCα as well. We generated six clones, with L309, N310, G312, V313, L316A, or K317 being individually substituted by an alanine (Fig. 8 A). In addition, we generated the construct PPARγ1 Δaa309-319, with helix 4 (aa309-319) being completely removed (Fig. 8 A). To prove the functionality of these constructs, we first verified their expression by Western blotting. As a control, the DsRed-PPARγ1 wild-type–encoding vector was included in the experiment.

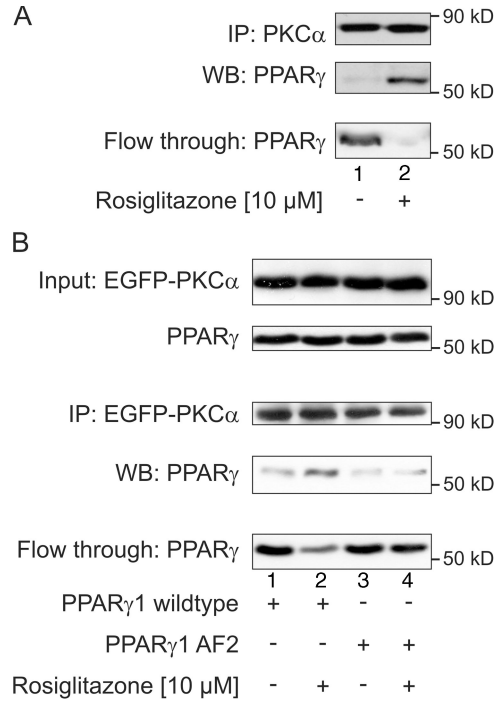

Figure 6. **PPARγ1 directly interacts with PKCα.** (A) THP-1 cells were differentiated for 24 h with 50 nM PMA. To allow new synthesis of PKCα, which is depleted in response to the differentation regime, cells were further cultured for 48 h in normal medium. Afterward, cells were treated for 1 h with 10 μM rosiglitazone or remained as controls. Cells were harvested and lysed, and PKCα was immunoprecipitated as described in Materials and methods. Eluates and flowthroughs were separated by Western blotting and stained for PPARγ and PKCα as indicated. (B) COS-7 cells were transiently cotransfected with PPARγ1 wild type/PKCα-EGFP or PPARγ1 AF2/PKCα-EGFP. 24 h later, cells were treated for 1 h with 10 μM rosiglitazone or remained as controls. Cells were harvested and lysed, and PKCα-EGFP was immunoprecipitated as described in Materials and methods. Input controls, eluates, and flowthroughs were separated by Western blotting and stained for PPARγ and PKCα as indicated. All experiments were performed at least three times, and representative data are shown.

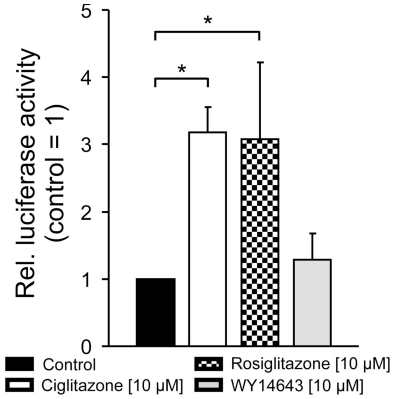

Figure 7. **PPARγ directly binds to PKCα.** COS-7 cells were transiently transfected with a combination of a target (PPARγ1), a bait (PKCα), and a reporter construct, as described in Materials and methods. Afterward, cells were treated with 10 μM ciglitazone, 10 μM rosiglitazone, 10 μM WY14643, or remained as controls. 6 h later, cells were harvested and lysed for a reporter analysis as described in Materials and methods. Experiments were performed at least three times in duplicate. *, $P < 0.05$. Data are the means ± the SD.

Because of a single aa exchange, or the 12 aa deletion, the molecular mass of proteins originating from the constructs remained unaltered compared with DsRed-PPARγ1 wild type when transfected into HEK293 cells (unpublished data).

To finally analyze the impact of the various mutations and the deletion on PKCα translocation, HEK293 cells were transiently cotransfected with the mutated/deleted PPARγ1 constructs tagged with DsRed-monomer, in combination with a PKCα-EGFP–encoding vector. PKCα localization was documented in cells that were untreated (Fig. 8, B and C, first rows), treated for 50 min with PMA (Fig. 8, B and C, second rows), treated for 1 h with rosiglitazone (Fig. 8, B and C, third rows), or preincubated for 1 h with rosiglitazone, followed by the addition of PMA for 50 min (Fig. 8, B and C, fourth rows). In cells transfected with one of the six constructs of the DsRed-tagged PPARγ1 mutations (L309A, N310A, and G312A [Fig. 8 B]; V313A, L316A, and K317A [Fig. 8 C]), PKCα-EGFP did not translocate to the cell membrane. A similar result was obtained in cells transfected with DsRed-PPARγ1 Δaa309-319 (Fig. 8 C, right), showing no PMA-mediated PKCα-EGFP translocation in rosiglitazone-pretreated cells. From these data, we conclude that helix 4 of the LBD is not involved in PPARγ1 binding to PKCα.

Based on these results, we decided to generate three PPARγ1 deletion constructs (DsRed-PPARγ1 aaΔ32-198, DsRed-PPARγ1 Δaa32-250, and DsRed-PPARγ1 Δaa51-406) with the belief that ligand binding is necessary for PPARγ1–PKCα interactions. As shown in Fig. 9 A, all deletions lack the DNA-binding domain (DBD) of PPARγ1. Furthermore, to characterize the role of the hinge domain in PKCα binding, it was eliminated to variable extents. In the DsRed-PPARγ1 Δaa32-198 construct, the first 26 aa of the hinge domain were deleted, and in the DsRed-PPARγ1 Δaa32-250 construct, 78 aa of the hinge domain were deleted. The hinge domain was completely removed in the DsRed-PPARγ1 Δaa51-406 construct. In this construct, a part of the LBD/AF2 domain was deleted as well (aa288-406). All constructs lack a part of the AF1 domain.

Expression of the cloned constructs was verified by Western blotting. As controls, the DsRed-PPARγ1 wild-type– and AF2 mutant–encoding vectors were included in the experiment. Estimated molecular mass of deletion construct proteins, transfected into HEK293 cells, were verified using an anti–red fluorescent protein antibody (Fig. 9 B). Taking into account that the DBD was removed, DNA binding and concomitant transactivation by corresponding PPARγ1 deletion constructs should be abolished. Therefore, we performed a set of reporter experiments, cotransfecting DsRed-PPARγ deletion constructs in combination with a PPRE-reporter plasmid into HEK293 cells. As expected, adding 10 μM rosiglitazone for 6 h to cells transfected with the PPARγ1 deletion constructs did not alter basal transactivation. In contrast, the DsRed PPARγ1 wild-type–encoding plasmid provoked a twofold induction of luciferase expression, whereas the DsRed PPARγ1 AF2 dominant-negative mutant blocked transactivation even below basal values, mediated by endogenous PPARγ in HEK293 cells (unpublished data).

To elucidate the role of these deletions on PKCα translocation, HEK293 cells were transiently cotransfected with the shortened DsRed-monomer–tagged PPARγ1 constructs in

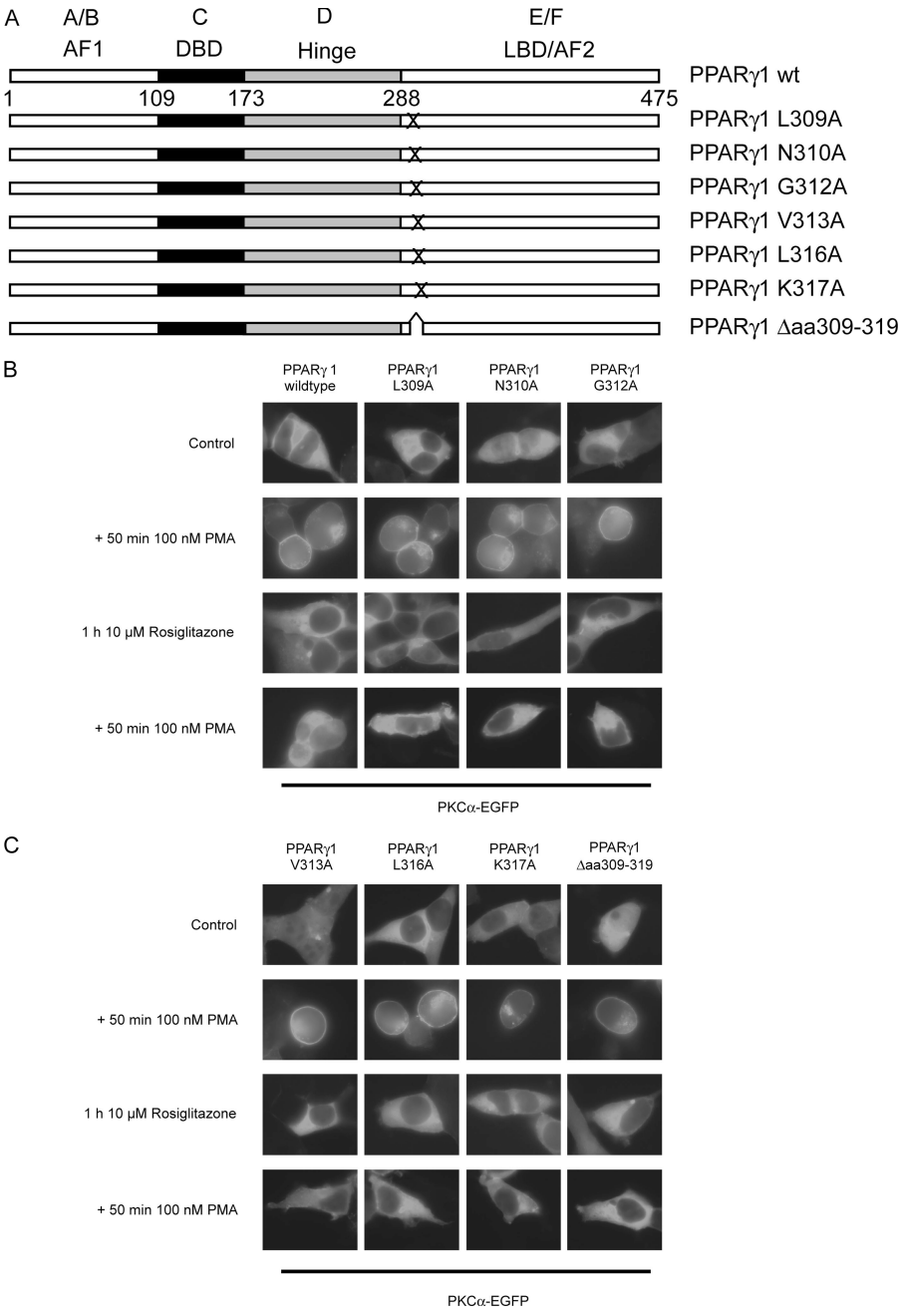

Figure 8. **Helix 4 of the LBD/AF2 domain does not mediate PPARγ binding to PKCα.** (A) Scheme of the PPARγ1 constructs. (B and C) HEK293 cells were cotransfected with DsRed-PPARγ1 wild type/PKCα-EGFP (B, first panel), DsRed-PPARγ1 L309A/PKCα-EGFP (B, second panel), DsRed-PPARγ1 N310A/PKCα-EGFP (B, third panel), DsRed-PPARγ1 G312A/PKCα-EGFP (B, fourth panel), PPARγ1 V313A/PKCα-EGFP (C, first panel), PPARγ1 L316A/PKCα-EGFP (C, second panel), PPARγ1 K317A/PKCα-EGFP (C, third panel) or DsRed-PPARγ1 Δaa309-319/PKCα-EGFP (C, fourth panel). To follow PKCα-EGFP localization, 24 h after transfection, cells were treated for 50 min with 100 nM PMA (second row), for 1 h with 10 μM rosiglitazone (third row), pretreated for 1 h with 10 μM rosiglitazone followed by the addition of 100 nM PMA for 50 min (fourth row) or remained as controls (first row). Experiments were performed three times, and representative data are shown.

combination with a PKCα-EGFP–encoding vector. To follow PKCα translocation, 100 nM PMA was added to (1 h, 10 μM) rosiglitazone-pretreated cells. PKCα localization was documented in untreated cells (Fig. 9 C, first row), cells treated for 50 min with PMA (Fig. 9 C, second row), for 1 h with rosiglitazone (Fig. 9 C, third row), or preincubated for 1 h with rosiglitazone, followed by the addition of PMA for 50 min (Fig. 9 C, fourth row). In cells transfected with the DsRed-tagged PPARγ1 Δaa32-198 construct, PKCα-EGFP did not translocate to the cell membrane. However, in cells expressing the DsRed-tagged PPARγ1 Δaa32-250 or Δaa51-406 construct, PKCα translocated to the cell membrane in response to 100 nM PMA.

From these data, we conclude that for PKCα, binding a part of the hinge domain of PPARγ1 is indispensable. To further narrow the involved region of PPARγ1, we finally created the construct DsRed-PPARγ1 Δaa206-224 (Fig. 10 A), containing a deletion of helix 1 (aa206-224) of PPARγ1, which is located in the hinge domain (aa173-288). Helix 1 has already been identified to mediate the protein–protein interaction of PPARγ with ERK5 (Akaike et al., 2004). Expression of the construct results as expected in protein, demonstrating a slightly reduced protein mass (Fig. 10 B, lane 2) because of the aa206-224 deletion compared with the DsRed-PPARγ1 wild type (Fig. 10 B, lane 1). We transiently cotransfected HEK cells with the PPARγ1 Δaa206-224 construct tagged with DsRed-monomer in combination with a PKCα-EGFP–encoding vector. In cells expressing the DsRed-tagged PPARγ1 Δaa206-224 (Fig. 10 C), PKCα translocated to the cell membrane in response to 100 nM PMA.

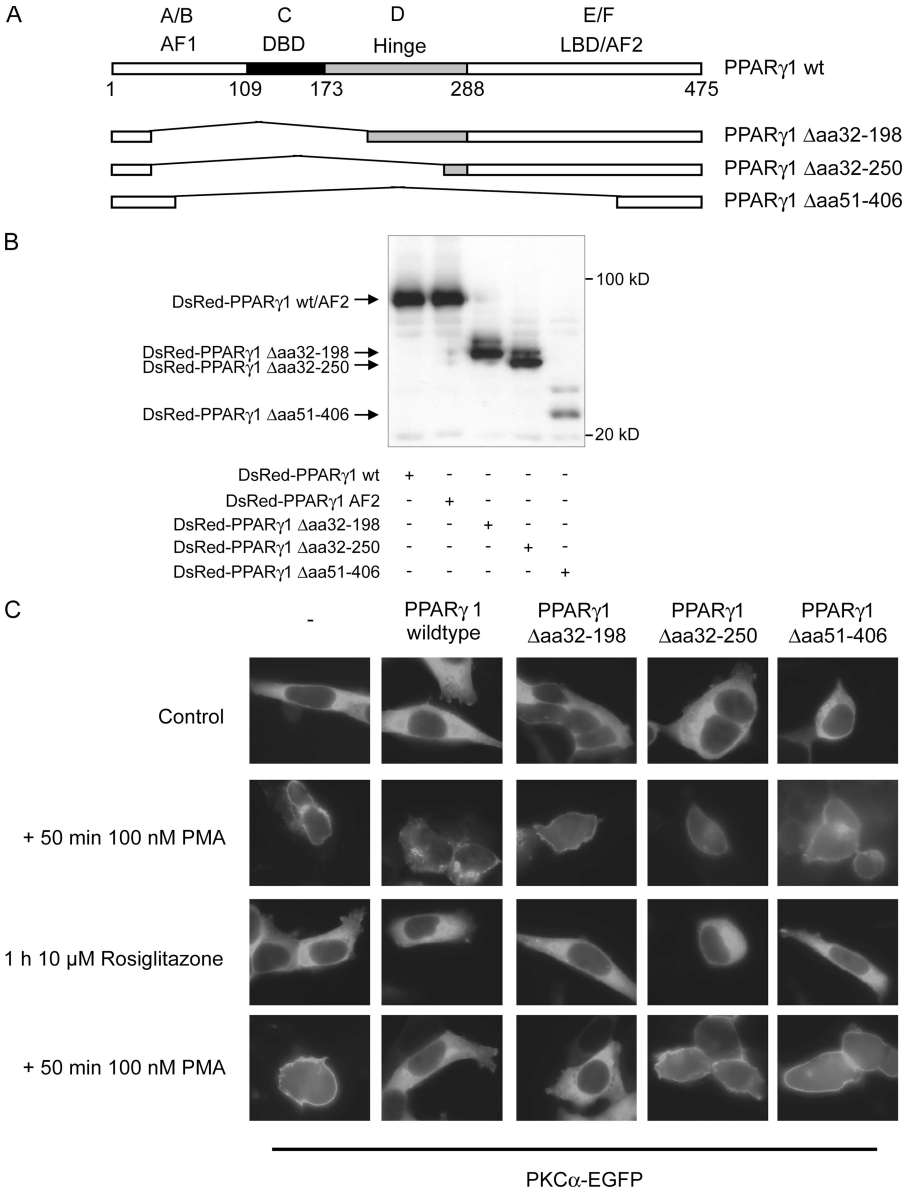

Figure 9. **Hinge domain mediates PPARγ1 binding to PKCα.** (A) Scheme of the PPARγ1 constructs. (B) HEK293 cells were transiently transfected with one of the PPARγ1 constructs, as indicated. 24 h after transfection cells were lysed. Western blotting was performed, and blots were stained for DsRed. All experiments were performed at least three times, and representative data are shown. (C) HEK293 cells were transfected with PKCα-EGFP only (first panel) or cotransfected with DsRed-PPARγ1 wild type/PKCα-EGFP (second panel), DsRed-PPARγ1 Δ32-198/PKCα-EGFP (third panel), DsRed-PPARγ1 Δ32-250/PKCα-EGFP (fourth panel), or DsRed-PPARγ1 Δ51-406/PKCα-EGFP (fifth panel). To follow PKCα-EGFP localization, 24 h after transfection, cells were treated for 50 min with 100 nM PMA (second row), treated for 1 h with 10 μM rosiglitazone (third row), pretreated for 1 h with 10 μM rosiglitazone followed by the addition of 100 nM PMA for 50 min (fourth row), or remained controls (first row). Experiments were performed three times, and representative data are shown.

We conclude that PPARγ1 binds to PKCα via the helix 1, which is located in the hinge domain of PPARγ1.

Discussion

Recently, we demonstrated that monocyte/macrophage desensitization at least partially attenuates PKCα signaling (von Knethen et al., 2005; Johann et al., 2006). We provide evidence that PPARγ agonists block PKCα translocation to the cell membrane and concomitant protein depletion, which normally occurs after cell activation. In monocytic cell lines, PPARγ expression has been previously described (McIntyre et al., 2003; Musiek et al., 2005; von Knethen et al., 2005), and it was verified using primary human monocyte–derived macrophages. These data corroborate the work of Tontonoz et al. (1998) and Chinetti et al. (1998), showing PPARγ expression in differentiated macrophages. However, even if PPARγ is expressed, PPARγ agonists are known to mediate PPARγ-dependent and -independent effects (Nosjean and Boutin, 2002). To this end, 15d-PGJ_2 has been described to directly modify H-ras, provoking a constitutively active enzyme (Oliva et al., 2003) or inhibiting I-κB kinase, and thus suppressing NF-κB signaling (Straus et al., 2000). Our approach, using cells expressing PPARγ1 wild type or the PPARγ1 agonist-binding mutant AF2, substantiates the need of PPARγ activation in our system. Only in cells expressing PPARγ1 wild type was translocation of PKCα blocked by PPARγ activation. The PPARγ1 AF2 mutant did not prevent PMA-mediated PKCα translocation. These data support the notion of a PPARγ-dependent mechanism.

PPARγ-mediated inhibition of classical PKCs has been previously described (Verrier et al., 2004). In their case, PKCβ translocation was blocked by PPARγ agonists via DGKα up-regulation. DGKα metabolizes DAG, which is an established activator of classical and novel PKC isoforms. Therefore, its induction/activation will remove the potential PKC activator, causing desensitization as seen in our experiments. However, in

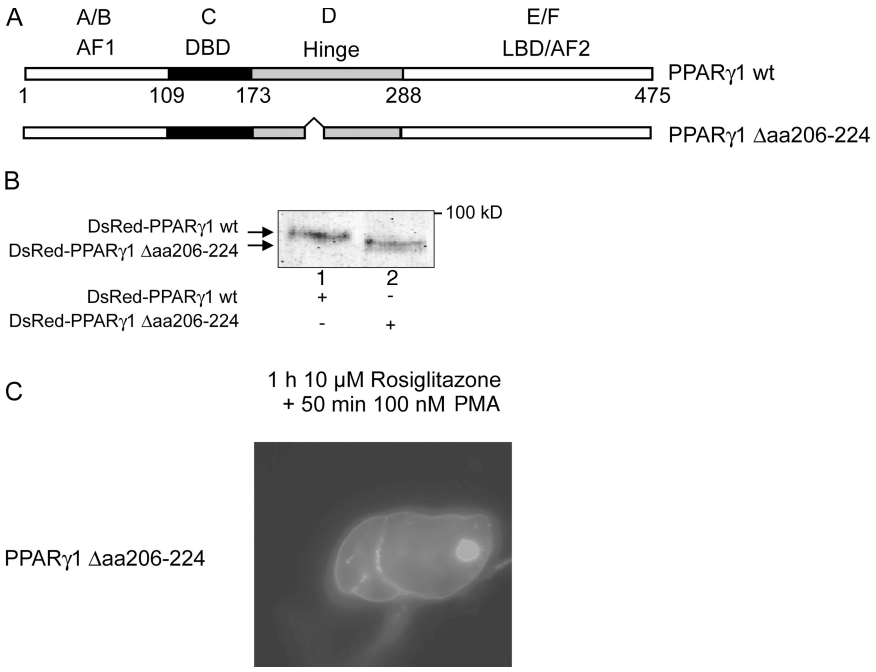

Figure 10. **Hinge helix 1 mediates PPARγ1 binding to PKCα.** (A) Scheme of the PPARγ1 construct. (B) HEK293 cells were transiently transfected with the DsRed-PPARγ1 wild type as control or the DsRed-PPARγ1 Δaa206-224 construct as indicated. 24 h after transfection, cells were lysed. Western blotting was performed, and blots were stained for DsRed. (C) HEK293 cells were cotransfected with DsRed-PPARγ1 Δaa206-224/PKCα-EGFP. 24 h after transfection, cells were treated for 1 h with 10 μM rosiglitazone. To follow PKCα-EGFP translocation, 100 nM PMA was added to cells, and localization of PKCα-EGFP was examined 50 min thereafter. Experiments were performed three times and representative data are shown.

our experiments, a role of DGKα up-regulation must be excluded because the protein-synthesis inhibitor CHX did not restore PKCα translocation. In line with this, our PPARγ1 Δaa32-198 construct, where the PPARγ1 DBD was removed, still inhibits PKCα translocation. Further support for our hypothesis, suggesting a direct PPARγ1–PKCα interaction in preventing PKCα translocation, came from previous studies (Johann et al., 2006). In this case, PPARγ was activated in response to apoptotic cells, attenuating PKCα translocation and concomitant ROS production. In this study, the role of PPARγ was verified using a PPARγ d/n cell line. In these cells, pretreatment with apoptotic cells left PMA-mediated PKCα translocation and subsequent ROS production unaltered. A premise for this assumption is that PPARγ is expressed at least partially in the cytosol. Generally, the nuclear hormone receptor PPARγ is described to be exclusively localized in the nucleus (Akiyama et al., 2002; Feige et al., 2005). In support of our hypothesis, suggesting cytoplasmatic localization as well, we noticed a minor amount of PPARγ1 to remain in the cytosol. This is based on results using DsRed-PPARγ1–transfected cells, as well as immunohistochemical detection of endogenous PPARγ1 located in the cytosol of RAW 264.7 macrophages besides its major nuclear localization. It should be noted that cytoplasmatic distribution of PPARγ is in line with the work of Abella et al. (2005). In their study, an approach similar to our experiments was used, with EGFP-tagged PPARγ used to characterize intracellular distribution of PPARγ. Results indicated that PPARγ is not exclusively located in the nucleus. Furthermore, localization of PPARγ in the cytoplasma in the promonocytic cell lines HL-60 and K-562 has been observed, especially in response to the PPARγ agonist troglitazone (Liu et al., 2005). This work was done using immunohistochemical detection of endogenous PPARγ. Therefore, side effects, such as unphysiological high expression or a modified protein behavior as a result of a tag or label (Feige et al., 2005), can be excluded. In addition, Burgermeister et al. (2006) recently provided evidence that PPARγ is actively exported from the nucleus into the cytosol in a MEK1-dependent manner, further supporting our observed PPARγ localization pattern. Furthermore, Patel et al. (2005) described cytoplasmatic localization of a different PPAR isoform, PPARα, when coexpressed with CAP350, which is a putative centrosome-associated protein of unknown function. Therefore, we propose that members of the PPAR family may localize in the cytoplasm, possibly after activation, when bound to cytoplasmic proteins such as PKCα. Immunoprecipitation of PKCα from lysates of differentiated THP-1 cells coimmunoprecipitated PPARγ. Remarkably, PPARγ1 coimmunoprecipitation was only seen once PPARγ1 became activated. The requirement of PPARγ1 activation was verified using an agonist-binding mutant of PPARγ1, which did not block PKCα translocation in response to PMA stimulation. A direct PPARγ1–PKCα interaction was further supported by a mammalian two-hybrid system with PPARγ1 as the target and PKCα as the bait construct, provoking luciferase reporter gene expression when target and bait proteins interact. To avoid autocrine activation of the reporter system, PPARγ has to be cloned as a target protein linked to the NF-κB transactivation domain, not allowing this hybrid protein to bind to the promoter of the reporter. However, DNA binding of PPARγ1 to PPREs, and concomitant scavenging the NF-κB-AD-PPARγ1 hybrid protein from the two-hybrid assay, cannot be excluded.

Based on the well-established role of helix 4 of the PPARγ LBD in mediating protein–protein interaction of PPARγ with coactivators, such as CBP and SRC-2, or repressors, such as the nuclear receptor corepressor and the silencing mediator for retinoic acid receptor and thyroid-hormone receptor (Nolte et al., 1998; Westin et al., 1998; Perissi et al., 1999; Perissi and Rosenfeld, 2005), we first generated 6 PPARγ1 constructs in which only

1 aa was exchanged and 1 construct in which helix 4 was completely removed. Unexpectedly, these constructs did not alter rosiglitazone-dependent inhibition of PKCα translocation.

Taking into account that PPARγ binding to other factors, such as adipocyte-type fatty acid–binding protein or extracellular signal-related kinase 5, which do not belong to the family of transcriptional coactivators, can be mediated by other PPARγ domains, such as A/B/C and D/E/F (Adida and Spener, 2006) or the hinge domain (domain D; Akaike et al., 2004), we created three PPARγ1 deletion constructs. All of them lack the entire DBD (domain C). In addition, different parts of the A/B and D domains have been removed, and one construct contained the C-terminal third of the E/F domains only. Based on our collective results, we provide evidence that a part of the hinge domain probably confers the PPARγ1–PKCα interaction, which is present in the PPARγ1 Δaa32-198 construct but absent in the Δaa32-250 construct, when PPARγ1 is activated by an agonist, thus requiring the LBD/AF2 domains. One known region of PPARγ1 located in aa198-250 is the hinge helix 1 (aa 206–224). Therefore, we cloned a PPARγ1 construct with helix 1deleted (DsRed- PPARγ1 Δaa206-224). In cells transfected with this construct, PKCα translocated even after rosiglitazone pretreatment in response to PMA. From these results, we conclude that PPARγ1 binds to PKCα via the hinge helix 1 domain, after PPARγ1 has been activated by a ligand.

The proposed mechanism of PPARγ1–PKCα binding proceeds fast. 1 h of prestimulation with PPARγ agonists is sufficient to inhibit PKCα translocation in response to 100 nM PMA. However, PKCα translocation by 1 μM PMA was not blocked. These results support the assumption that the capacity of cytoplasmatic PPARγ to bind PKCα correlates with the strength of PKCα activation. Likely, very strong activation signals, such as 1 μM PMA, exceed the inhibitory impact of PPARγ. Thus, the role of PPARγ in blocking PKCα signaling might be only transient, allowing PKCα activation by a more stringent activator. This makes the mechanism more interesting for the development of new therapy strategies. Prolonged periods of PPARγ activation, which provoke transcriptional control to target members of the NADPH oxidase system, have already been described ($p22^{phox}$, $p47^{phox}$, and $gp91^{phox}$; Inoue et al., 2001; von Knethen and Brune, 2002; Hwang et al., 2005). Consequently, in these cells PPARγ contributes to an antiinflammatory phenotype by blocking NADPH oxidase-dependent ROS production.

An involvement of PPARγ in attenuating inflammatory reactions to improve the clinical picture of sepsis has previously been shown (for review see Zingarelli and Cook, 2005). In line with this, our results add to this data. In our system, PMA-mediated NF-κB activation was inhibited in response to PPARγ agonist pretreatment to 50% in RAW 264.7 cells, as well as primary human macrophages. In accordance, PMA-induced TNF-α expression was PPARγ dependently reduced to 70%. It has been observed that PPARγ activation inhibits multiple organ failure in an animal model (Abdelrahman et al., 2005), although the underlying mechanism remains unclear. The option to adjust a pro- versus antiinflammatory monocyte/macrophage phenotype will provide new possibilities for the development of therapies to control systemic inflammation. Our data add a new antiinflammatory role for PPARγ based on the ability to scavenge PKCα in the cytosol, thus, blocking membrane translocation and downstream signaling.

Materials and methods

Monocyte isolation

We analyzed human cells from peripheral blood of healthy donors. For monocyte enrichment, we isolated PBMCs from donors using Ficoll-Hypaque gradients (PAA Laboratories). Cells were left to adhere on culture dishes (Primaria 3072; Becton Dickinson) for 60 min at 37°C. Nonadherent cells were removed. Afterward, cells were differentiated to macrophages by culturing them in complete RPMI containing 10% AB-positive human serum. Flow cytometry confirmed that the monocyte-like population was 90–95% pure ($CD14^+$ vs. $CD14^-$).

Cell culture

We cultivated RAW 264.7 and THP-1 in RPMI 1640 (PAA Laboratories). HEK293 and COS-7 cells were cultured in DME high glucose (PAA Laboratories). Both media were supplemented with 100 U/ml penicillin (PAA Laboratories), 100 μg/ml streptomycin (PAA Laboratories), and 10% heat-inactivated fetal calf serum (PAA Laboratories). Ciglitazone (Biomol), rosiglitazone (Biomol), WY14643 (Biomol), and CHX (Sigma-Aldrich) were dissolved in DMSO. Appropriate vehicle controls were performed.

Immunofluorescence staining

To determine intracellular PPARγ localization, we seeded RAW 264.7 macrophages directly on a slide. After 24 h, cells were treated as indicated and fixed on the slides by 1-h incubation in 4% paraformaldehyde at 4°C. Thereafter, cells were permeabilized in PBS containing 0.2% Triton X-100 for 15 min. After a washing step in PBS, cells were incubated for 2 h with a 1:250 dilution of a rabbit α-PPARγ antibody (Calbiochem) at 4°C. After three 5-min washing steps with PBS, cells were incubated with a secondary goat α-rabbit antibody (1:250) labeled with Alexa Fluor 546 (Invitrogen) for 2 h at 4°C. Cells were incubated for 2 h with a 1:250 dilution of a mouse α-PKCα antibody (BD Biosciences) at 4°C. After three 5-min washing steps with PBS, cells were incubated with a secondary goat α-mouse antibody (1:250) labeled with Alexa Fluor 488 (Invitrogen) for 2 h at 4°C. Again, cells were washed three times with PBS and counterstained with DAPI (1 μg/ml in PBS for 15 min). After a final 5-min washing step in PBS, cells were covered with Vectashield mounting medium (Linaris) and a coverslip. PPARγ and PKCα localization were determined using an AxioScope fluorescence microscope with the ApoTome upgrade (Carl Zeiss MicroImaging, Inc.; lens 63×/0.6 NA; ocular 10×) at room temperature, documented by a charge-coupled device camera (Carl Zeiss MicroImaging, Inc.) and AxioVision Software (Carl Zeiss MicroImaging, Inc.).

Vector construction, transient transfection, fluorescence microscopy, and reporter analysis

To examine cellular PPARγ localization, we subcloned human PPARγ1 into the DsRed-monomer–encoding vector pDsRed-Monomer-C1 (CLONTECH Laboratories, Inc.) using the infusion ligation kit (CLONTECH Laboratories, Inc.). To allow integration of the PPARγ1 fragment, the vector was cut within the multicloning site (MCS) by BamHI and XhoI. To insert PPARγ1 (provided by V.K.K. Chatterjee, University of Cambridge, Cambridge, UK), we used the pcDNA3-PPARγ1 wild-type and AF2 vectors for PPARγ1 amplification by PCR, using the following sequences based on the infusion ligation requirements (changed nucleotides are underlined): wild type, 5′-GGACTCAGATCTCGAATGGTTGACACAGAGATC GCATTCTG-3′ and 3′-AGGACGTCCTCTAGATGTTCCTGAACATGCTAGGTGGCCT AGA T-5′; AF2 mutant, 5′-GGACTCAGATCTCGAATGGTTGACACAGAGATCGCAT-TCTG-3′ and 3′-GAGACGTCCGCTAGATGTTCCTGAACATGCTAGGTGG-CCT AGAT-5′. Annealing temperatures were 62°C for the first cycle and 72°C for the later ones and calculated using the Oligo software (MBI). Infusion reaction of the cleaved vector with the amplified PPARγ1 wild-type or AF2 fragment was performed according to the distributor's instructions.

Site-directed mutagenesis to generate single aa exchanges (L309A, N310A, G312A, V313A, L316A, K317A) and deletion of helix 1 (aa206-224) or 4 (aa309-319) of PPARγ1 were performed using the QuikChange XLII kit (Stratagene). The following primers were used (changed nucleotides are underlined): L309A, 5′-CCTGGTTTTGTAAATC-TTGACGCGAACGACCAAGTAACTCTCCTC-3′ and 5′-GAGGAGAGT-

TACTTGGTCGTTCGCGTCAAGATTTACTTTTCCAGG-3′; N310A, 5′-CC TGGTTTTGTAAATCTTGACTTGGCGGACCAAGTAACTCTCCTC-3′ and 5′-GAGGAGAG TTACTTGGTCCGCCAAGTCAAGATTTACTTTTCCAGG-3′; G312A, 5′-GTAAATCTTG ACTTGAACGACGCGGTAACTCTCCTCAAA-TATGG-3′ and 5′-CCATATTTGAGGAGAGT TACCGCGTCGTTCAAGTC-AAGATTTAC-3′; V313A, 5′-GTAAATCTTGACTTGAACGA CCAAGCGAC-TCTCCTCAAATATGG-3′ and 5′-CCATATTTGAGGAGAGTCGCTTGGTCG-TTCAAGTCAAGATTTAC-3′; L316A, 5′-CTTGAACGACCAAGTAACTCTC-GCGAAAT ATGGAGTCCACGAG-3′ and 5′-CTCGTGGACTCCATATTT-CGCGAGAGTTACTTGGTCG TTCAAG-3′; K317A, 5′-CTTGAACGACC-AAGTAACTCTCCTCGCGTATGGAGTCCAC GAG-3′ and 5′-CTCGTGG-ACTCCATACGCGAGGAGAGTTACTTGGTCGTTCAAG-3′; Δaa309-319, 5′-CCTGGTTTTGTAAATCTTGACCCGCTGACCAAAGCAAAG-3′ and 5′-CTTT GCTTTGGTCAGCGGGTCAAGATTTACAAAACCAGG-3′. The pcDNA3-PPARγ1 wild-type vector was used as a template. An initial denaturation step was performed at 95°C for 1 min, followed by 18 cycles at 95°C for 50 s, annealing at 60°C for 50 s, and extension at 68°C for 7 min. A final extension phase was performed at 68°C for 7 min.

DsRed-PPARγ1 Δaa32-198 was constructed by deleting the EcoRV fragment in the DsRed-PPARγ1 wild-type vector. DsRed-PPARγ1 Δaa32-250 was constructed by deleting the EcoRV–EcoRI fragment in the DsRed-PPARγ1 wild-type vector, blunting the sticky EcoRI end before religating the remaining plasmid. Finally, DsRed-PPARγ1 Δaa51-406 was constructed by deleting the XmnI fragment in the DsRed-PPARγ1 wild-type vector. Restriction enzymes were obtained from New England Biolabs. The Klenow fragment and T4 ligase were provided by Fermentas. All manipulations did not alter the open reading frame of PPARγ1.

Correct orientation and sequence of the generated vectors was verified by restriction analyses and/or sequencing. The PKCα-EGFP signaling sample (pPKCα-EGFP) used was obtained from CLONTECH Laboratories, Inc.

To follow PKCα translocation and PPARγ distribution, HEK293 cells were seeded directly onto a slide, and then transiently transfected by $CaPO_4$-precipitation with combinations of pDsRed-Monomer-C1 PPARγ1 wild type/pPKCα-EGFP, pDsRed-Monomer-C1 PPARγ1 AF2/pPKCα-EGFP, or the generated deletion and mutation constructs together with pPKCα-EGFP. 24 h after transfection, cells were used for experiments. Cells were treated as indicated. Afterward, cells were fixed on the slides by 1-h incubation in 4% paraformaldehyde at 4°C. Cells were washed three times with PBS and counterstained with DAPI (1 μg/ml in PBS for 15 min). After a final 5-min washing step in PBS, cells were covered with Vectashield mounting medium and a coverslip. Translocation of PKCα-EGFP and DsRed-PPARγ1 wild type/AF2 distribution was analyzed using an AxioScope fluorescence microscope with the ApoTome upgrade (lens 63×/0.6 NA; ocular 10×) at room temperature, documented by a charge-coupled device camera and the AxioVision Software.

For reporter analysis, HEK293 cells were transiently transfected by $CaPO_4$-precipitation with pDsRed-Monomer-C1 PPARγ1 wild-type, -AF2, Δaa32-198, Δ32-250, Δ51-406 constructs, or the empty DsRed vector in combination with the PPRE-containing $p(AOX)_3$-TK-luc reporter plasmid. Transfection efficiency was normalized by cotransfecting a pRL-TK control vector encoding for *Renilla reniformis* luciferase. Transfections were performed in duplicate, and each experiment was repeated at least three times.

Coimmunoprecipitation

After THP-1, cells were differentiated for 24 h with 50 nM PMA, PMA was removed, and cells were incubated for an additional 48 h in complete medium. Afterward, cells were stimulated for 1 h with 10 μM rosiglitazone or remained as controls. Eventually, cells were harvested and lysed in lysis buffer (50 mM Tris, 5 mM EDTA, 150 mM NaCl, 0.5% Nonidet-40, and 1 mM PMSF, pH 8.0). To assure cell lysis, cells were sheared 10 times with a 16-gauge needle, followed by a brief 10-s sonication (Sonifier; Branson; duty cycle 100%, output control 60%). Cell debris was removed by centrifugation (10,000 *g* for 5 min), and 1 mg of protein was used for immunoprecipitation. Sample volume was adjusted with lysis buffer to 1 ml. 2 μg anti-PKCα antibody (BD Biosciences) was added and incubated at 4°C overnight. Thereafter, 50 μl μMACS protein A microbeads (Miltenyi Biotech) were added and incubated for 6 h. Lysate was applied onto an equilibrated μ column, which was already placed in the magnetic field of a μMACS separator. The flowthrough was collected and saved for further analysis. The column was rinsed 4 times with 200 μl wash buffer (150 mM NaCl, 1% Igepal CA-630, 0.5% sodium deoxycholate, 0.1% SDS, and 50 mM Tris HCl, pH 8.0), followed by 2 washes with low ionic buffer (20 mM TrisHCl, pH 7.5). Afterward, the column was removed from the magnetic field and the remaining proteins were eluted using 50 μl of lysis buffer.

COS-7 cells were transiently transfected by electroporation (450 V/300 μF; Equibio Easyjet T Prima; Peqlab) with a combination of pcDNA3 PPARγ1 wild-type or pcDNA3-PPARγ1 AF2 and pPKCα-EGFP. Immunoprecipitation was performed as described in the previous paragraph using μMACS anti–GFP-microbeads (Miltenyi Biotec)

Mammalian two-hybrid assay

To use PPARγ1 and PKCα in the mammalian two-hybrid system (Stratagene), PPARγ1 was cloned into the BamHI–HindIII site of the pCMV-AD MCS, and PKCα was cloned into the BamHI–HindIII site of the pCMV-BD MCS. PPARγ was amplified from the pcDNA3-PPARγ1 wild-type vector and PKCα from the vector pPKCα-EGFP. The following primers were used: pCMV-BD-PPARγ1, 5′-GCCGGAA TTGGGATCCATGGTTGACACAGAGA-TGCCATTCTG-3′ and 5′-ACGCGGCCGCAAGC TCTAGTACAAGTCCTT-GTAGATCTCCTGCAGG-3′; pCMV-AD-PKCα, 5′-CAGCGGCC AAGGAT-CCATGGCTGACGTTTTCCCGGG-3′ and 5′-ACGCGGCCGCAAGC-TTCATA CTGCACTCTGTAAGATGGGGTGC-3′. Annealing temperatures were 62°C for the first cycle and 72°C for the later ones, and were calculated using the Oligo software (MBI). Infusion reaction of the BamHI–HindIII–cleaved vectors with the amplified PPARγ1 wild-type- or PKCα-fragment was performed according to the distributor's instructions. Correct orientation and sequence of the generated vectors was verified by restriction analyses and sequencing. COS-7 cells were transiently transfected by electroporation using a combination of the two constructed vectors, as well as the pFR-luciferase reporter vector (Stratagene). Afterward, cells were incubated for 24 h, and then stimulated for 6 h with 10 μM ciglitazone, 10 μM rosiglitazone, or 10 μM WY14643, or they remained as controls. Thereafter, cells were lysed and assayed for firefly luciferase activity by a luciferase assay (Promega).

Western blot analysis

Cell lysis was achieved with lysis buffer (50 mM Tris, 5 mM EDTA, 150 mM NaCl, 0.5% Nonidet-40, and 1 mM PMSF, pH 8.0) and 20-s sonication (Sonifier; duty cycle 100%, output control 60%). Whole-cell lysates were cleared by centrifugation (10,000 *g* for 5 min), and protein concentration was determined with the Lowry method. 80 μg of protein was resolved on 10% polyacrylamide gels and blotted onto nitrocellulose sheets, basically following standard methodology. Equal loading and correct protein transfer to nitrocellulose was routinely quantitated by Ponceau S staining. Filters were incubated with the anti-PKCα antibody (1:500; BD Biosciences), anti-PPARγ antibody (1:500; Santa Cruz Biotechnology, Inc.), anti-RFP antibody (1:1,000; MBL), or anti-actin antibody (1:2,000; GE Healthcare) overnight at 4°C. Horseradish peroxidase–conjugated polyclonal antibodies (1:5,000; GE Healthcare) were used for enhanced chemiluminescence detection.

Quantification of TNF-α expression

Supernatants from RAW 264.7 macrophages treated as indicated were harvested after the indicated times. Content of TNF-α was quantified using the BD Cytometric Bead Array TNF-α Flex Set (BD Biosciences) according to the supplier's instructions using a FACSCanto flowcytometer. Interpretation of the results was performed with the FCAP Array software (Soft Flow, Inc./BD Biosciences).

EMSA

Nuclear extracts were prepared as previously described (von Knethen and Brune, 2001). An established EMSA method, with slight modifications, was used (Camandola et al., 1996). Nuclear protein (20 μg) was incubated for 30 min at room temperature with 2 μg poly(dI-dC) from GE Healthcare, 2 μl buffer D (20 mM Hepes/KOH, 20% glycerol, 100 mM KCl, 0.5 mM EDTA, 0.25% Nonidet P-40, 2 mM DTT, and 0.5 mM PMSF, pH 7.9), 4 μl buffer F (20% Ficoll-400, 100 mM Hepes/KOH, 300 mM KCl, 10 mM DTT, and 0.5 mM PMSF, pH 7.9), and 250 fmol 5′-IRD700–labeled oligonucleotide (Metabion) in a final volume of 20 μl. Specific p65 and p50 supershift antibodies (2 μg; Santa Cruz Biotechnology, Heidelberg, Germany) were added as indicated. DNA–protein complexes were resolved at 80 V for 1 h in a native 6% polyacrylamide gel, and visualized with the Odyssey infrared imaging system (LI-COR). Oligonucleotides with the consensus NF-κB site (bold letters) were used (Peng et al., 1995): 5′-GCCAGTTGA **GGGGACTTTCC**CAGGC-3′; 3′-CGGTCAACT**CC-CCTGAAAG G**GTCCG-5′.

Statistical analysis

Each experiment was performed at least three times. Statistical analysis was performed using the paired *t* test. We considered P values ≤ 0.05 as significant. Otherwise, representative data are shown.

We thank Nadja Wallner for expert technical assistance.

This work was supported by grants from the Deutsche Forschungsgemeinschaft (Br999).

Submitted: 5 May 2006
Accepted: 24 January 2007

References

Abdelrahman, M., A. Sivarajah, and C. Thiemermann. 2005. Beneficial effects of PPAR-gamma ligands in ischemia-reperfusion injury, inflammation and shock. *Cardiovasc. Res.* 65:772–781.

Abella, A., P. Dubus, M. Malumbres, S.G. Rane, H. Kiyokawa, A. Sicard, F. Vignon, D. Langin, M. Barbacid, and L. Fajas. 2005. Cdk4 promotes adipogenesis through PPARgamma activation. *Cell Metab*. 2:239–249.

Adida, A., and F. Spener. 2006. Adipocyte-type fatty acid-binding protein as inter-compartmental shuttle for peroxisome proliferator activated receptor gamma agonists in cultured cell. *Biochim. Biophys. Acta*. 1761:172–181.

Akaike, M., W. Che, N.L. Marmarosh, S. Ohta, M. Osawa, B. Ding, B.C. Berk, C. Yan, and J. Abe. 2004. The hinge-helix 1 region of peroxisome proliferator-activated receptor gamma1 (PPARgamma1) mediates interaction with extracellular signal-regulated kinase 5 and PPARgamma1 transcriptional activation: involvement in flow-induced PPARgamma activation in endothelial cells. *Mol. Cell. Biol.* 24:8691–8704.

Akiyama, T.E., C.T. Baumann, S. Sakai, G.L. Hager, and F.J. Gonzalez. 2002. Selective intranuclear redistribution of PPAR isoforms by RXR alpha. *Mol. Endocrinol.* 16:707–721.

Altiok, S., M. Xu, and B.M. Spiegelman. 1997. PPARgamma induces cell cycle withdrawal: inhibition of E2F/DP DNA-binding activity via down-regulation of PP2A. *Genes Dev.* 11:1987–1998.

Burgermeister, E., D. Chuderland, T. Hanoch, M. Meyer, M. Liscovitch, and R. Seger. Interaction with MEK causes nuclear export and downregulation of PPARgamma. 2006. *Mol. Cell. Biol.* DOI:10.1128/MCB.00601-06.

Camandola, S., G. Leonarduzzi, T. Musso, L. Varesio, R. Carini, A. Scavazza, E. Chiarpotto, P.A. Baeuerle, and G. Poli. 1996. Nuclear factor kB is activated by arachidonic acid but not by eicosapentaenoic acid. *Biochem. Biophys. Res. Commun.* 229:643–647.

Chinetti, G., S. Griglio, M. Antonucci, I.P. Torra, P. Delerive, Z. Majd, J.C. Fruchart, J. Chapman, J. Najib, and B. Staels. 1998. Activation of proliferator-activated receptors alpha and gamma induces apoptosis of human monocyte-derived macrophages. *J. Biol. Chem.* 273:25573–25580.

Chung, S.W., B.Y. Kang, and T.S. Kim. 2003. Inhibition of interleukin-4 production in CD4+ T cells by peroxisome proliferator-activated receptor-gamma (PPAR-gamma) ligands: involvement of physical association between PPAR-gamma and the nuclear factor of activated T cells transcription factor. *Mol. Pharmacol.* 64:1169–1179.

Desreumaux, P., L. Dubuquoy, S. Nutten, M. Peuchmaur, W. Englaro, K. Schoonjans, B. Derijard, B. Desvergne, W. Wahli, P. Chambon, et al. 2001. Attenuation of colon inflammation through activators of the retinoid X receptor (RXR)/peroxisome proliferator-activated receptor gamma (PPARgamma) heterodimer. A basis for new therapeutic strategies. *J. Exp. Med.* 193:827–838.

Docke, W.D., F. Randow, U. Syrbe, D. Krausch, K. Asadullah, P. Reinke, H.D. Volk, and W. Kox. 1997. Monocyte deactivation in septic patients: restoration by IFN-gamma treatment. *Nat. Med.* 3:678–681.

Feige, J.N., L. Gelman, C. Tudor, Y. Engelborghs, W. Wahli, and B. Desvergne. 2005. Fluorescence imaging reveals the nuclear behavior of peroxisome proliferator-activated receptor/retinoid X receptor heterodimers in the absence and presence of ligand. *J. Biol. Chem.* 280:17880–17890.

Gurnell, M., J.M. Wentworth, M. Agostini, M. Adams, T.N. Collingwood, C. Provenzano, P.O. Browne, O. Rajanayagam, T.P. Burris, J.W. Schwabe, et al. 2000. A dominant-negative peroxisome proliferator-activated receptor gamma (PPARgamma) mutant is a constitutive repressor and inhibits PPARgamma-mediated adipogenesis. *J. Biol. Chem.* 275:5754–5759.

Han, S., N. Sidell, P.B. Fisher, and J. Roman. 2004. Up-regulation of p21 gene expression by peroxisome proliferator-activated receptor gamma in human lung carcinoma cells. *Clin. Cancer Res.* 10:1911–1919.

Hansson, G.K. 2005. Inflammation, atherosclerosis, and coronary artery disease. *N. Engl. J. Med.* 352:1685–1695.

Hotchkiss, R.S., and I.E. Karl. 2003. The pathophysiology and treatment of sepsis. *N. Engl. J. Med.* 348:138–150.

Hwang, J., D.J. Kleinhenz, B. Lassegue, K.K. Griendling, S. Dikalov, and C.M. Hart. 2005. Peroxisome proliferator-activated receptor-gamma ligands regulate endothelial membrane superoxide production. *Am. J. Physiol. Cell Physiol.* 288:C899–C905.

Ikeda, Y., A. Sugawara, Y. Taniyama, A. Uruno, K. Igarashi, S. Arima, S. Ito, and K. Takeuchi. 2000. Suppression of rat thromboxane synthase gene transcription by peroxisome proliferator-activated receptor gamma in macrophages via an interaction with NRF2. *J. Biol. Chem.* 275:33142–33150.

Inoue, I., S. Goto, T. Matsunaga, T. Nakajima, T. Awata, S. Hokari, T. Komoda, and S. Katayama. 2001. The ligands/activators for peroxisome proliferator-activated receptor alpha (PPARalpha) and PPARgamma increase Cu2+,Zn2+-superoxide dismutase and decrease p22phox message expressions in primary endothelial cells. *Metabolism*. 50:3–11.

Johann, A.M., A. von Knethen, D. Lindemann, and B. Brune. 2006. Recognition of apoptotic cells by macrophages activates the peroxisome proliferator-activated receptor-gamma and attenuates the oxidative burst. *Cell Death Differ.* 13:1533–1540.

Kalechman, Y., U. Gafter, R. Gal, G. Rushkin, D. Yan, M. Albeck, and B. Sredni. 2002. Anti-IL-10 therapeutic strategy using the immunomodulator AS101 in protecting mice from sepsis-induced death: dependence on timing of immunomodulating intervention. *J. Immunol.* 169:384–392.

Kobayashi, Y., S. Ueki, G. Mahemuti, T. Chiba, H. Oyamada, N. Saito, A. Kanda, H. Kayaba, and J. Chihara. 2005. Physiological levels of 15-deoxy-Delta12,14-prostaglandin J2 prime eotaxin-induced chemotaxis on human eosinophils through peroxisome proliferator-activated receptor-gamma ligation. *J. Immunol.* 175:5744–5750.

Leesnitzer, L.M., D.J. Parks, R.K. Bledsoe, J.E. Cobb, J.L. Collins, T.G. Consler, R.G. Davis, E.A. Hull-Ryde, J.M. Lenhard, L. Patel, et al. 2002. Functional consequences of cysteine modification in the ligand binding sites of peroxisome proliferator activated receptors by GW9662. *Biochemistry*. 41:6640–6650.

Liew, F.Y., D. Xu, E.K. Brint, and L.A. O'Neill. 2005. Negative regulation of toll-like receptor-mediated immune responses. *Nat. Rev. Immunol.* 5:446–458.

Liu, J., H. Lu, R. Huang, D. Lin, X. Wu, Q. Lin, J. Zheng, X. Pan, J. Peng, Y. Song, et al. 2005. Peroxisome proliferator activated receptor-gamma ligands induced cell growth inhibition and its influence on matrix metalloproteinase activity in human myeloid leukemia cells. *Cancer Chemother. Pharmacol.* 56:400–408.

Liu, W.S., and C.A. Heckman. 1998. The sevenfold way of PKC regulation. *Cell. Signal.* 10:529–542.

McIntyre, T.M., A.V. Pontsler, A.R. Silva, A. St Hilaire, Y. Xu, J.C. Hinshaw, G.A. Zimmerman, K. Hama, J. Aoki, H. Arai, and G.D. Prestwich. 2003. Identification of an intracellular receptor for lysophosphatidic acid (LPA): LPA is a transcellular PPARgamma agonist. *Proc. Natl. Acad. Sci. USA*. 100:131–136.

Musiek, E.S., L. Gao, G.L. Milne, W. Han, M.B. Everhart, D. Wang, M.G. Backlund, R.N. Dubois, G. Zanoni, G. Vidari, et al. 2005. Cyclopentenone isoprostanes inhibit the inflammatory response in macrophages. *J. Biol. Chem.* 280:35562–35570.

Nolte, R.T., G.B. Wisely, S. Westin, J.E. Cobb, M.H. Lambert, R. Kurokawa, M.G. Rosenfeld, T.M. Willson, C.K. Glass, and M.V. Milburn. 1998. Ligand binding and co-activator assembly of the peroxisome proliferator-activated receptor-gamma. *Nature*. 395:137–143.

Nosjean, O., and J.A. Boutin. 2002. Natural ligands of PPARgamma: are prostaglandin J(2) derivatives really playing the part? *Cell. Signal.* 14:573–583.

Oliva, J.L., D. Perez-Sala, A. Castrillo, N. Martinez, F.J. Canada, L. Bosca, and J.M. Rojas. 2003. The cyclopentenone 15-deoxy-delta 12,14-prostaglandin J2 binds to and activates H-Ras. *Proc. Natl. Acad. Sci. USA*. 100:4772–4777.

Pascual, G., A.L. Fong, S. Ogawa, A. Gamliel, A.C. Li, V. Perissi, D.W. Rose, T.M. Willson, M.G. Rosenfeld, and C.K. Glass. 2005. A SUMOylation-dependent pathway mediates transrepression of inflammatory response genes by PPAR-gamma. *Nature*. 437:759–763.

Patel, H., R. Truant, R.A. Rachubinski, and J.P. Capone. 2005. Activity and subcellular compartmentalization of peroxisome proliferator-activated receptor alpha are altered by the centrosome-associated protein CAP350. *J. Cell Sci.* 118:175–186.

Peng, H.B., P. Libby, and J.K. Liao. 1995. Induction and stabilization of I kappa B alpha by nitric oxide mediates inhibition of NF-kappa B. *J. Biol. Chem.* 270:14214–14219.

Perissi, V., and M.G. Rosenfeld. 2005. Controlling nuclear receptors: the circular logic of cofactor cycles. *Nat. Rev. Mol. Cell Biol.* 6:542–554.

Perissi, V., L.M. Staszewski, E.M. McInerney, R. Kurokawa, A. Krones, D.W. Rose, M.H. Lambert, M.V. Milburn, C.K. Glass, and M.G. Rosenfeld. 1999. Molecular determinants of nuclear receptor-corepressor interaction. *Genes Dev.* 13:3198–3208.

Rogler, G. 2006. Significance of anti-inflammatory effects of PPARgamma agonists? *Gut*. 55:1067–1069.

Straus, D.S., G. Pascual, M. Li, J.S. Welch, M. Ricote, C.H. Hsiang, L.L. Sengchanthalangsy, G. Ghosh, and C.K. Glass. 2000. 15-deoxy-delta

12,14-prostaglandin J2 inhibits multiple steps in the NF-kappa B signaling pathway. *Proc. Natl. Acad. Sci. USA*. 97:4844–4849.

Tontonoz, P., L. Nagy, J.G. Alvarez, V.A. Thomazy, and R.M. Evans. 1998. PPARgamma promotes monocyte/macrophage differentiation and uptake of oxidized LDL. *Cell*. 93:241–252.

Verrier, E., L. Wang, C. Wadham, N. Albanese, C. Hahn, J.R. Gamble, V.K. Chatterjee, M.A. Vadas, and P. Xia. 2004. PPARgamma agonists ameliorate endothelial cell activation via inhibition of diacylglycerol-protein kinase C signaling pathway: role of diacylglycerol kinase. *Circ. Res.* 94:1515–1522.

von Knethen, A., and B. Brune. 2001. Delayed activation of PPARgamma by LPS and IFN-gamma attenuates the oxidative burst in macrophages. *FASEB J.* 15:535–544.

von Knethen, A., and B. Brune. 2002. Activation of peroxisome proliferator-activated receptor gamma by nitric oxide in monocytes/macrophages down-regulates p47phox and attenuates the respiratory burst. *J. Immunol.* 169:2619–2626.

von Knethen, A., A. Tautenhahn, H. Link, D. Lindemann, and B. Brune. 2005. Activation-induced depletion of protein kinase C alpha provokes desensitization of monocytes/macrophages in sepsis. *J. Immunol.* 174:4960–4965.

Wang, L.H., X.Y. Yang, X. Zhang, J. Huang, J. Hou, J. Li, H. Xiong, K. Mihalic, H. Zhu, W. Xiao, and W.L. Farrar. 2004. Transcriptional inactivation of STAT3 by PPARgamma suppresses IL-6-responsive multiple myeloma cells. *Immunity*. 20:205–218.

Wang, P., P.O. Anderson, S. Chen, K.M. Paulsson, H.O. Sjogren, and S. Li. 2001. Inhibition of the transcription factors AP-1 and NF-kappaB in CD4 T cells by peroxisome proliferator-activated receptor gamma ligands. *Int. Immunopharmacol.* 1:803–812.

Westin, S., R. Kurokawa, R.T. Nolte, G.B. Wisely, E.M. McInerney, D.W. Rose, M.V. Milburn, M.G. Rosenfeld, and C.K. Glass. 1998. Interactions controlling the assembly of nuclear-receptor heterodimers and co-activators. *Nature*. 395:199–202.

Yang, W., C. Rachez, and L.P. Freedman. 2000. Discrete roles for peroxisome proliferator-activated receptor gamma and retinoid X receptor in recruiting nuclear receptor coactivators. *Mol. Cell. Biol.* 20:8008–8017.

Zingarelli, B., and J.A. Cook. 2005. Peroxisome proliferator-activated receptor-gamma is a new therapeutic target in sepsis and inflammation. *Shock*. 23:393–399